Supplementary Information for "Two-dimensional half-metals MSi_2N_4 (M=Al, Ga, In, Tl) with intrinsic *p*-type ferromagnetism and ultrawide bandgap"

Yi-min Ding,[a*⋆] Yiqi Huo, [b⋆] Gaojing Fang, [ac] Luo Yan,[ab] Yu Wu,[a*] and Liujiang Zhou[ab*]

[a] Yangtze Delta Region Institute (Huzhou), University of Electronic Science and Technology of China, Huzhou 313001, China

[b] School of Physics, University of Electronic Science and Technology of China, Chengdu 610054, China

[c] School of Electronic Science and Engineering, University of Electronic Science and Technology of China, Chengdu 610054, China

⋆ Yi-min Ding and Yiqi Huo contributed equally to this work

(Email: ymding00@qq.com(Y.-M Ding); 291320917@qq.com(Y. Wu);ljzhou86@uestc.edu.cn(L. Zhou))

1. Methodology of calculation of the Curie temperature.

The Heisenberg model with the Metropolis Monte Carlo method provides an accurate description with continuous degrees of freedom while effective and universal spin update algorithms remain highly desirable. In SEU-mtc program,[1] new algorithms for the magnetization switching in the classical Heisenberg model based on the concept of Euler angles and quaternion, which update the spins simply by a rotation matrix and convert to sphere and Cartesian coordinates in a very convenient way.

For the systemsthat only consider the nearest-neighbor and the nextnearest-neighbor situation, and the easy-to-magnetic axis is clearly in the z-axis, the Hamiltonian can be written in this form,

$$H = -J_1\sum_{\langle i,j\rangle}\vec{s}_i\vec{s}_j - J_2\sum_{\langle i,k\rangle}\vec{s}_i\vec{s}_k - \sum_i A_i^z\vec{s}_i^z\vec{s}_i^z$$

In this work, we assume that $\vec{s} = \frac{1}{2}\vec{M}$ and the basic structure of the grid is {x, y, z, i}. When the simulation is performed, the original cell is expanded into supercells and {x, y, z} are the index of the original cell in the supercell. As the supercell retains as a periodic structure, it should be chosen as large as possible to ensure the diversity and validity of the simulation, similar to the simulations of periodic molecular dynamics. Since computer performance and time are limited, it is necessary to select a suitable supercell size and improve computational efficiency. When the simulation is initiated, a random vector is randomly selected from the grid and generates a new trial vector to replace it, and the energy difference $\Delta E = E_{new}-E_{init}$ with the new vector is calculated. Then the parameter $p = \exp(\Delta E/(k_BT))$ is computed as the probability of accepting this trial vector. When $\Delta E < 0$, the ratio p is greater than 1, indicating the trial vector could replace the initially selected vector. If the trial vector is not accepted, the initially selected vector will not be changed. Therefore, the probability ratio can be written in this form,

$$p = \begin{cases} \exp\left(-\frac{\Delta E}{k_BT}\right), & when\Delta E > 0 \\ 1, & when\Delta E < 0 \end{cases}$$

The main part of the Metropolis Monte Carlo simulation is to repeat the above steps until the system reaches an equilibrium state and then continues to repeat several loops to collect the statistics

observables. Internal energy can be invoked as a criterion for determining the equilibrium state. In this work, four observations will be collected, the internal energy E, the magnetic moment M, the specific heat capacity C, and the magnetic susceptibility χ as defined below.

$$E = \langle E \rangle = \frac{1}{\mathcal{N}} \sum_i H_i$$

$$M = \langle \vec{M} \rangle = \frac{1}{\mathcal{N}} \left| \sum_i \vec{M}_i \right|$$

$$C = \frac{\partial E}{\partial T} = \frac{(\Delta E)^2}{k_B T} = \frac{\langle E^2 \rangle - \langle E \rangle^2}{k_B T^2}$$

$$\chi = \frac{\partial M}{\partial T} = \frac{\left(\Delta \vec{M}\right)^2}{k_B T} = \frac{\langle \vec{M}^2 \rangle - \langle \vec{M} \rangle^2}{k_B T}$$

The spin update process can be seen as random walks (RW) on the surface of the sphere. In fact, the random walk in the MMC can be treated as a rotation process as seen in the 3D rotation group (often denoted SO(3)). Therein Euler angles and quaternion, which are the most commonly used methods for description structures in 3D rendering software, can provide an efficient solution. Taking advantage of the Euler angle, spin updates can be easily operated by a rotation matrix R. The coordinates of the spin states, both sphere and Cartesian coordinate, after each spin update can be obtained and stored in the meantime. Benefiting from the concise definition and converting function, quaternions avoid using the trigonometric function and thus save runtime memory consumption and reduce computation time. Furthermore, the quaternion and Euler angles can be converted to each other directly, which are beneficial to later framework conversion.[2]

2. Calculation of the exchange parameters J.

For $AlSi_2N_4$ and $GaSi_2N_4$, the exchange parameters J are calculated based on the following equations:

$$\begin{cases} E_{FM}=-12J_1S^2-24J_2S^2+E_0 \\ E_{AFM\text{-}1}=12J_1S^2-24J_2S^2+E_0 \\ E_{AFM\text{-}2}=4J_1S^2+8J_2S^2+E_0 \end{cases}$$

For $InSi_2N_4$ and $TlSi_2N_4$, the exchange parameters J are calculated based on the following equations:

$$\begin{cases} E_{FM}=-24J_1S^2-12J_2S^2+E_0 \\ E_{AFM\text{-}1}=-24J_1S^2+12J_2S^2+E_0 \\ E_{AFM\text{-}2}=8J_1S^2+4J_2S^2+E_0 \end{cases}$$

Table S1: Energy difference between different configurations. Energy of most stable configuration is set as zero.

ΔE (eV)	**α_1**	**α_2**	**α_3**	**β_1**	**β_2**	**β_3**	**β_4**	**γ_1**	**γ_2**	**γ_3**	**γ_4**
$AlSi_2N_4$	0.864	0.849	0.83	0.009	0.020	0	0.009	0.701	0.698	0.691	0.690
$GaSi_2N_4$	0.634	0.631	0.634	0.014	0.015	0	0.014	0.482	0.503	0.477	0.500
$InSi_2N_4$	0.264	0.262	0.251	0.012	0	0.009	0.014	1.133	1.133	1.139	1.133
$TlSi_2N_4$	0.114	0.106	0.220	0.033	0	0.064	0.032	0.846	0.823	0.858	0.833
$MoSi_2N_4$	0.171	0.083	0	1.165	1.265	1.259	1.165	2.554	2.665	2.460	2.590

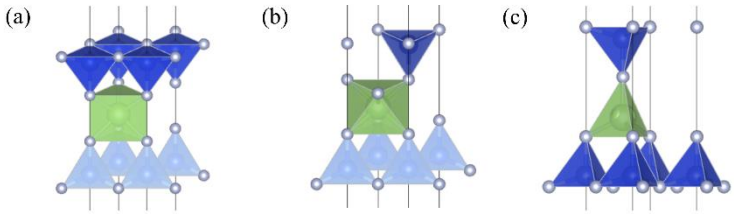

Figure S1: Three types of phases, α (a), β (b), γ (c) of MSi_2N_4 (M=Al,Ga,In,Tl).

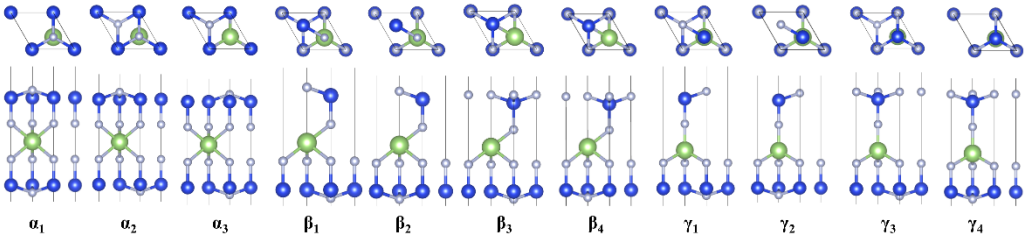

Figure S2: Eleven possible configurations of MSi_2N_4.

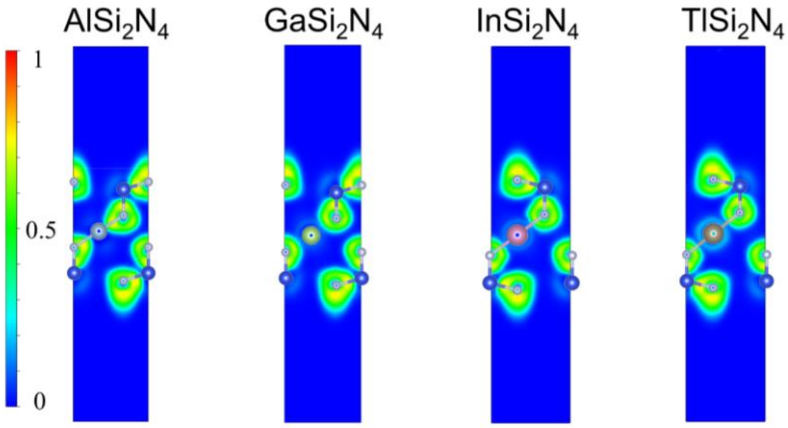

Figure S3: The electron localization function (ELF) plots of MSi_2N_4.

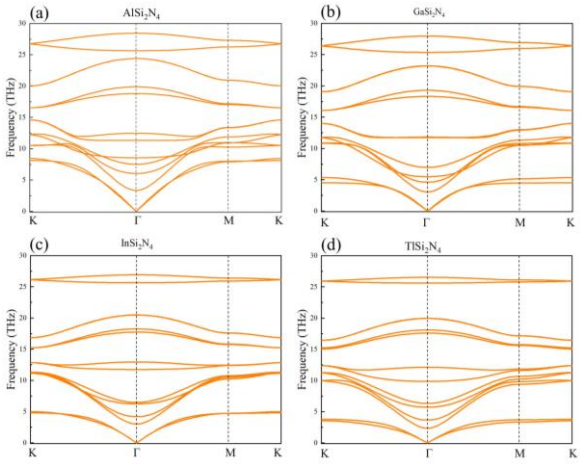

Figure S4: The phonon spectra of (a) $AlSi_2N_4$, (b) $GaSi_2N_4$, (c) $InSi_2N_4$ and (d) $TlSi_2N_4$.

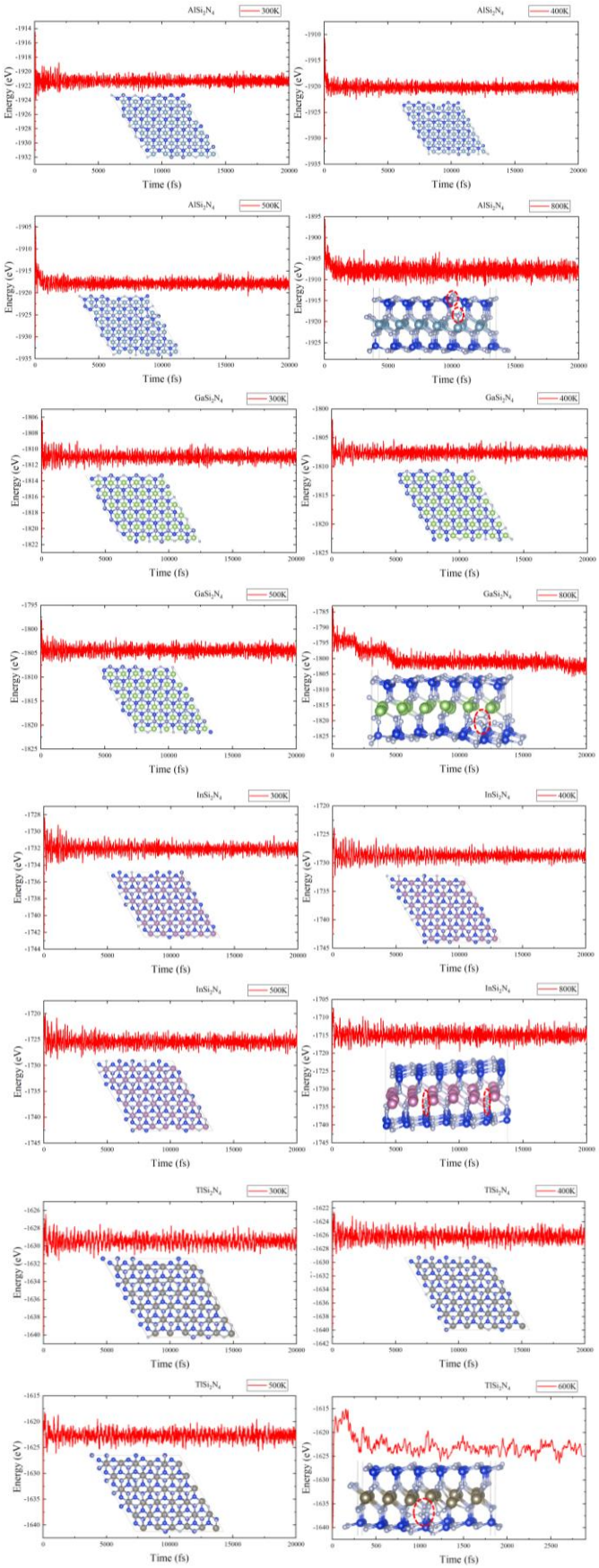

Figure S5: Energy variations at different temperatures under the AIMD simulations of $AlSi_2N_4$, $GaSi_2N_4$, $InSi_2N_4$ and $TlSi_2N_4$. The structure distortion is indicated by red dashed circle.

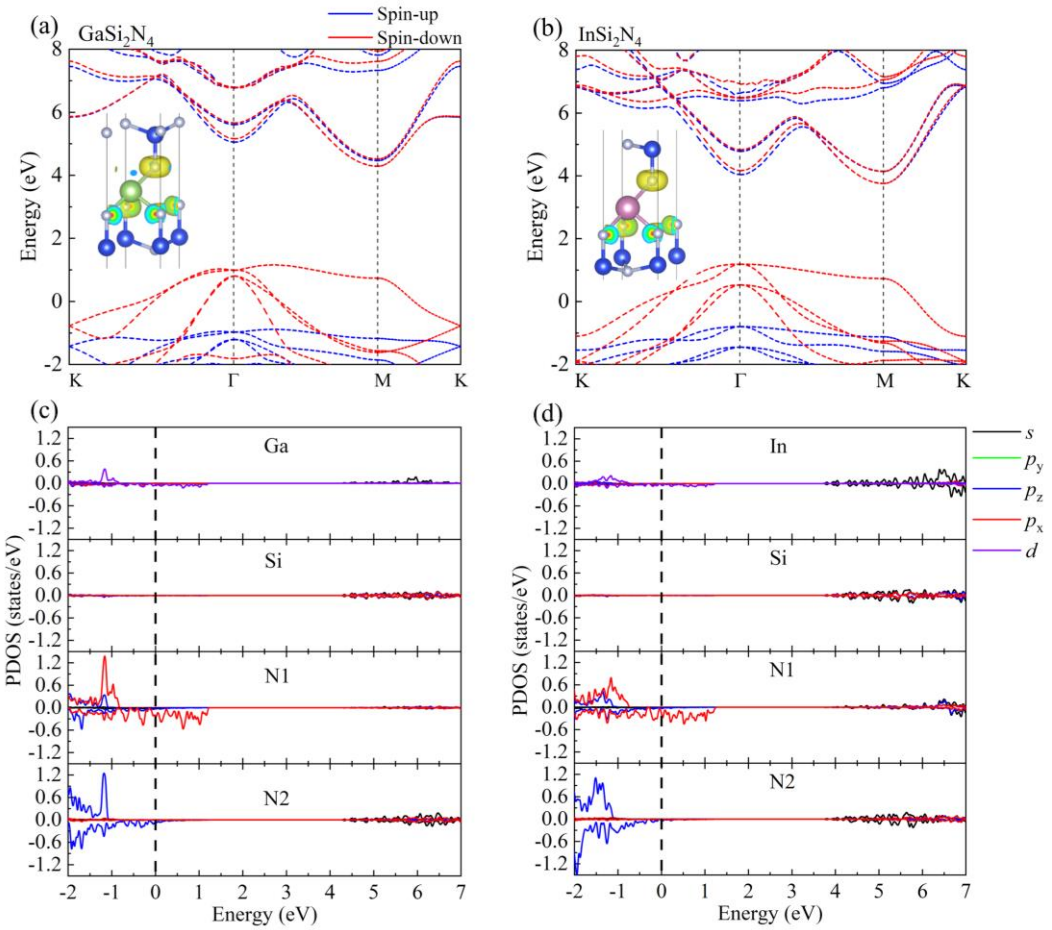

Figure S6: The spin-polarized band structure and projected density of states (PDOS) of (a)/(c) $GaSi_2N_4$ and (b)/(d) $InSi_2N_4$ from HSE06 functional. The Fermi energy is set to 0 eV. The inset shows the net magnetic charge density.

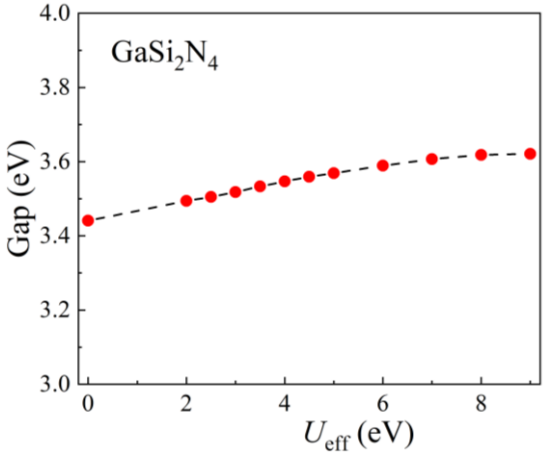

Figure S7: Spin-up band gap variation with U_{eff} for $GaSi_2N_4$.

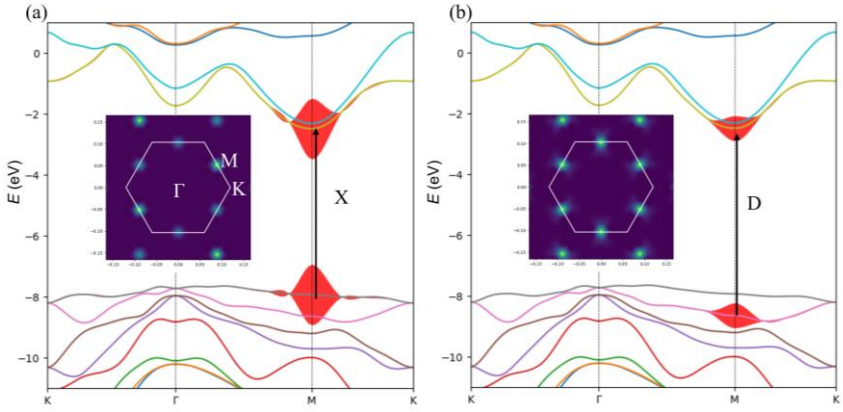

Figure S8: Plotting of the coefficients of the exciton wave functions projected over the DFT bands: (a) dark exciton X and (b) bright exciton D for $GaSi_2N_4$. Inset shows the coefficients of the exciton wave functions in k-space, and the white hexagon indicates the first brillouin zone.

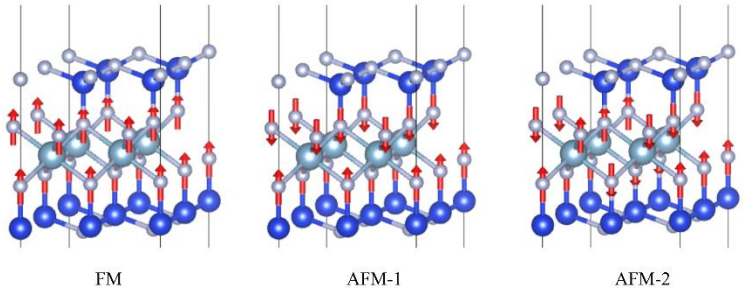

Figure S9: Three magnetic phases of FM, zigzag antiferromagnetic AFM-1 and armchair AFM-2.

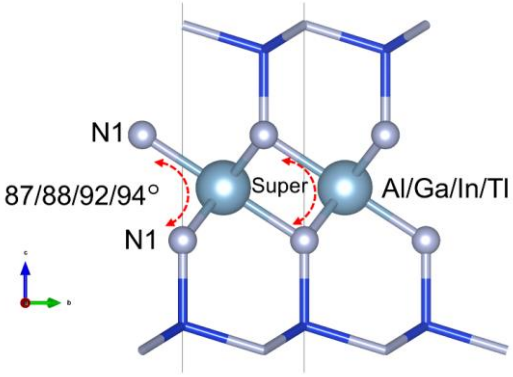

Figure S10: Illustrations of the N1–N1 super-exchange interactions and interlayer angles between the N1-M-N1 bond.

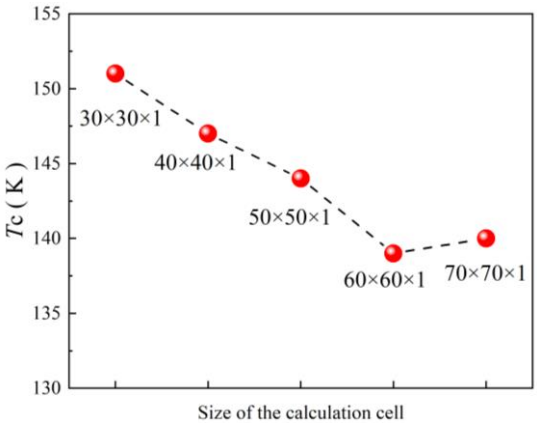

Figure S11: Critical temperature variation with the size of calculation cell.

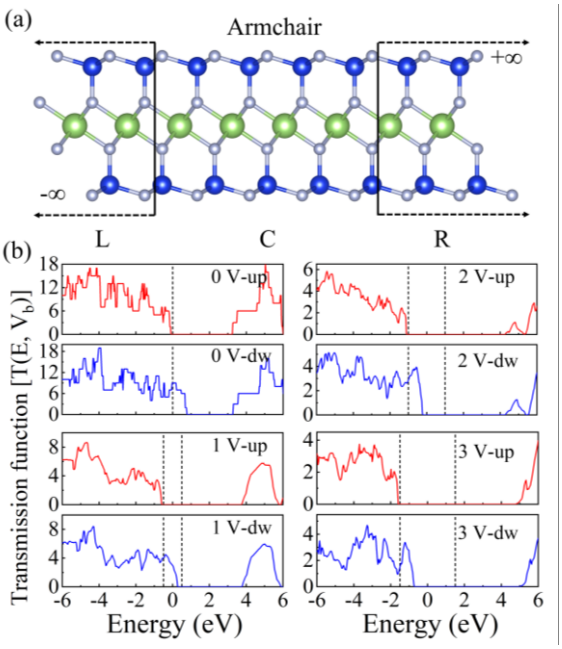

Figure S12: (a) Structural representation for the $GaSi_2N_4$ device along armchair direction. Spin resolved transmission functions along armchair direction at (b) zero, 1, 2 and 3 bias voltages. Black dotted lines indicate the bias window ($-V_b/2$, $+V_b/2$). The Fermi energy is set at zero energy.

References

1. Y. Zhang, B. Wang, Y. Guo, Q. Li and J. Wang, A universal framework for metropolis Monte Carlo simulation of magnetic Curie temperature, *Computational Materials Science*, 2021, **197**, 110638.

2. J. Diebel, Representing attitude: Euler angles, unit quaternions, and rotation vectors, *Matrix*. 2006, **58**, 1–35.